The Journal of Global Radiology

ENSURING MEDICAL IMAGING ACCESS FOR ALL

ORIGINAL RESEARCH

Validation of a Locally Designed Computed Tomography Dose Phantom: A Comparison Study with a Standard Acrylic Phantom in South-South, Nigeria

Anwuli Christiana Tobi[1], Chukwuka Emmanuel Mokobia[1], Joyce Ekeme Ikubor[2], Akintayo Daniel Omojola[3]

1. Department of Physics, Delta State University Abraka, Delta State, Nigeria
2. Department of Radiology, Faculty of Clinical Medicine, College of Health Sciences, Delta State University, Abraka, Nigeria
3. Department of Radiology, Medical Physics Unit, Federal Medical Centre Asaba, Delta State, Nigeria

* **Corresponding author.** Current address: Anwuli Christiana Tobi, Department of Physics, Delta State University, Abraka, Delta State, Nigeria, email: anwulitobi@gmail.com

DOI: 10.7191/jgr.2021.1118

Published: 4/16/2021

Citation: Tobi AC, Mokobia CE, Ikubor JE, Omojola AD. Validation of a locally designed computed tomography dose phantom: a comparison study with a standard acrylic phantom in South-South, Nigeria. J Glob Radiol. 2021;7(1):1118.

Keywords: Polymethymethacrylate, Volume Computed Tomography Dose Index, thermoluminescent dosimeter, phantom, dose length product, peripheries, absorbed dose

Word count: 3,131

Abstract

Purpose: The aim of this study was to determine the mean volume computed tomography dose index ($CTDI_{vol}$) for the standard head and body phantoms and locally designed head and body phantoms respectively. Similarly, this study determined and compared the displayed mean $CTDI_{vol}$ and Dose Length Product (DLP) for the above phantoms from the CT monitor. In addition, the percentage deviations of both phantoms were compared with the recommended limits from the International Atomic Energy Agency (IAEA) and the American College of Radiologists (ACR).

Materials and Methods: Dose measurements were made using a standard polymethymethacrylate (PMMA) phantom for head and body as well as a locally designed phantom with four CT scanners using thermoluminescence dosimeters (TLDs). The locally designed phantoms were made using a PMMA sheet, which was bent to give the desired cylindrical shape and was made like the standard phantoms. The constructed phantom was filled with water and the TLD chips were inserted into the center and peripheries of the phantoms to obtain the absorbed doses.

Results: The $CTDI_{vol}$ for the standard head and body phantom for center A was 66.97 and 21.85mGy and for B was 23.39 and 6.29mGy respectively. Similarly, the $CTDI_{vol}$ for the constructed head and body phantom for center A was 63.91 and 19.84mGy and for B was 24.67 and 6.30mGy respectively. The uncertainty between the standard and constructed head phantoms for centers A and B was 4.6 and 5.5% respectively, while that of the standard and constructed body phantoms for centers A and B was 9.2 and 0.0% respectively. The maximum percent deviation from the console $CTDI_{vol}$ and DLP values with the four phantoms for centers A and B was within ±20%. The mean correction factors for the head and body were 0.998 and 1.05 respectively.

Conclusion: The uncertainties obtained in this study were within the IAEA and ACR recommended value of ±20%. The constructed phantom proved useful for CT dose measurements.

Introduction

Computed tomography (CT) has been identified as a powerful tool in clinical diagnosis and management [1]. The advancement in the development of CT scanners has given rise to an increase in the application of this medical imaging modality [2]. The use of this application is on a high and continuous increase [3, 4]. In Nigeria, Adejoh et al. observed a significant increase in the use of CT scanners [5]. A fall out of this increased usage is a corresponding increase in radiation dose delivery to the patient relative to that from other imaging modalities [6]. For instance, the National Cancer Institute bulletin indicated that the ionizing radiation dose delivered from the use of CT could be 50 - 500 times higher than that from an X-ray chest examination [7, 8]. There has been concern that such high doses from this observed increase in the application of this diagnostic tool may in the long-term pose a significant cancer risk to the populace. This consequent increase in dose delivery may be attributable to inefficient optimization of scanner radiographic practices or to substandard/poor equipment conditions. It is therefore expected that appropriate examination conditions and procedures need to be optimized so as satisfy the twin purposes of good diagnostic quality and appropriate patient dose. The United Nations Scientific Committee on the Effects of Atomic Radiation (UNSCEAR) has documented that a number of evaluations on the doses associated with CT scans have been carried out and that these investigations were as a result of some observed incidences of overexposure to radiation [9]. In our study, the mean volume computed tomography dose index ($CTDI_{vol}$) was determined for the standard head and body phantom as well as the locally designed head and body phantom. Also, evaluation and comparison of console displayed $CTDI_{vol}$ and DLP values were made for the above phantoms. This is to verify the dose delivery accuracies in head and body CT scans in some available scanners in the South-South region of Nigeria.

Materials and Methods

Before the commencement of this study, ethical clearance was obtained from the Health Research and Ethics Committee from the four CT centers within the South-South region of Nigeria. Two were government-based and the other two were privately owned centers, located in Edo and Delta States, and coded as A, B, C, and D respectively. Some details of the scanners are given in Table 1.

Figure 1. A standard PMMA phantom with head (inner) and body.

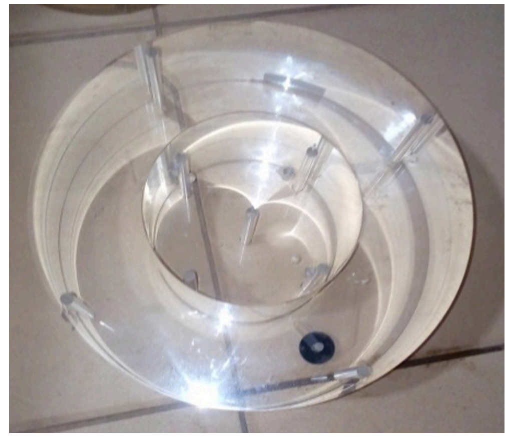

Figure 2. Constructed head (left) and body (right) phantom.

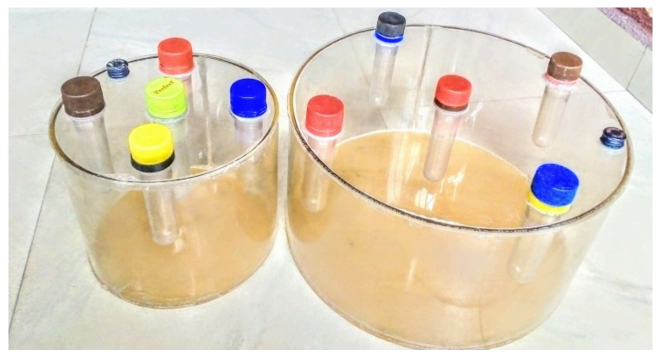

The PMMA phantom (Figure 1) was sourced from the National Institute of Radiation Protection and Research (NIRPR) in Ibadan, Nigeria. It was made up of two PMMA cylinders with a diameter of 16 and 32cm for the head and body respectively. Each of the cylinders had a length of 15cm. The cylinders had inserts large enough to accommodate the TLDs. The designed phantom was made in line with the design in Akpochafor et al. [10] (Figure 2). A PMMA sheet of thickness of 3×10^{-3}m and density of 1185 kgm^{-3} was manufactured to give the desired cylindrical shape and was made to meet the requirements as specified in the standard phantom. The constructed phantom was filled with water before inserting the TLD chips for measurement [11, 12]. Measurement was done using the

Table 1. Technical characteristics of the CT scanners.

Center	Scanner model	Manufacturer	Installation date	Slice	Scan mode
A	Aquillion	Toshiba	2009	64	Helical
B	Revolution ACTs	GE	2017	8	Helical/Axial
C	Light speed Plus	GE	2012	4	Helical/Axial
D	Bright speed	GE	2007	4	Helical/Axial

same protocol for both the standard and locally constructed phantom. Each center used different protocols for head and body. Comparison of dose measurements was made between the standard and constructed phantoms in centers A and B only. This is due to the downtime of the CT scanners in centers C and D when the standard phantoms were available for use. The displayed console doses were also compared using the constructed phantom on all the centers (A, B, C and D).

The average weighted computed tomography dose index $CTDI_w$ was determined by inserting the TLD chips in the center and peripheries. The $CTDI_w$ values were obtained from the relationship [13]:

$$CTDI_w = \frac{1}{3} CTDI_{centre} + \frac{2}{3} CTDI_{periphery} \quad (1)$$

Where $CTDI_{center}$ represents the mean dose measurements at the center of the standard head and body of a PMMA phantom.

$CTDI_{periphery}$ represents the mean dose of the measurements at four locations around the periphery of the standard head and body of a PMMA phantom.

The $CTDI_{vol}$ values were estimated using the expression in European Union EU given as [14]:

$$CTDI_{vol} = \frac{CTDI_w}{Pitch} \quad (2)$$

Where the "pitch" denotes the ratio between increment per rotation and beam width.

In addition, the Dose Length Product (DLP) was computed as [14]:

$$DLP = CTDI_{vol} \times \text{Scan length} \quad (3)$$

$CTDI_{vol}$ is primarily useful as a quality assurance tool to compare doses from different protocols and to compare scanner outputs from different manufacturers. This is to help us estimate the doses delivered to the 32 and 16cm head and body phantom [15]. The measured values from the constructed phantom were then validated against those of the standard phantom using the formula:

$$\%\ Deviation = \frac{\Delta D}{D_{SH/SB}} \times 100 \quad (4)$$

$\Delta D = D_{SH/SB} — D_{CH/CB}$ is the deviation of the TLD dose reading in the standard head (SH)/ body (SB) and the constructed head (CH)/ body (CB) phantoms.

A correction factor was determined for the designed head and body phantom in relation to the Standard PMMA phantoms. This is given as:

$$\text{Correction factor (k)} = \frac{Mean\ dose\ for\ standard\ PMMA\ phantom}{Mean\ dose\ for\ constructed\ phantom}$$

Statistical analysis

The data analysis was performed using SPSS for Windows, Version 20.0 (SPSS Inc., Chicago, IL, USA). Descriptive and independent sample t-test was used at a 95% level of significance. P<0.05 was considered statistically significant.

Results

Scan protocols for both adult head and abdomen phantom were set at potential tube voltage of 120kvp for all centers while the tube current varied amongst the scanners.

A total of four (4) models were used in this study, with three (3) from the same manufacturer. The number of slices of the CT ranged from 4-64 slices with axial and helical modes [Table 1]. The parameters for determining dose (mGy) were kVp, mAs, slice thickness, pitch, scan length and rotation time. The parameters for this study were statistically different from a one-way ANOVA ($P < 0.001$) [Table 2].

The $CTDI_{vol}$ for the standard head for center A and B were 66.97 and 23.39mGy and that of the standard body for center A and B were 21.85 and 6.29mGy respectively. The $CTDI_{vol}$ for the constructed head phantom for center A-D were 63.91, 24.67, 9.57 and 27.16mGy respectively, and for the constructed body were 19.84, 6.3, 6.98, and 7.12mGy respectively. An independent sample t-test shows that there were no differences between the mean dose for centers A and B for both head ($P = 0.870$) and body ($P = 0.766$) phantoms [Table 3].

The percent deviation in $CTDI_{vol}$ for the standard phantom (SP) and constructed phantom (CP) for the head in center A and B were 4.6 and 5.5% respectively and the body were 9.20 and 0.00% respectively [Table 4]. The correction factor (k) between the PMMA and constructed phantom for the head and body was around one.

There was no difference in the estimated dose to the head between the SP and CP ($P = 0.948$), and the estimated dose to the body between the SP and CP ($P = 0.901$) [Table 4].

The percent deviation in $CTDI_{vol}$ in the control console for the standard phantom (SP) and constructed phantom (CP) for the head in centers A and B were 4.6 and 4.3% respectively and the body were 0.00 and 2.65% respectively. The percent deviation in DLP in the control console for the standard phantom (SP) and constructed phantom (CP) for the head in center A and B were 20.4 and 10.25% respectively and the body were -8.55 and 2.72% respectively. In addition, the $CTDI_{vol}$ in the control console for both phantoms for the head in centers A and B was statistically the same ($P = 0.955$). The $CTDI_{vol}$ in the control console for both phantoms for the body in centers A and B was statistically the same ($P = 0.993$). The DLP in the control console for both phantoms for the head in centers A and B was statistically the same ($P = 0.857$). The DLP in the control console for both phantoms for the body in centers A and B was statistically the same ($P = 0.950$) [Table 5].

Table 2. Technical parameters of the scanners for standard and constructed phantoms.

Technical parameters	Phantom Specification			
	Standard head	Constructed head	Standard body	Constructed body
Center A				
Kv	120	120	120	120
mA	300	300	300	300
Slice Thickness (unit)	5	5	5	5
Scan mode	Helical	Helical	Helical	Helical
Pitch (unit)	0.64	0.64	0.83	0.83
Scan length (mm)	160	160	310	310
Rotation time (s)	0.75	0.75	0.50	0.50
Center B				
Kv	120	120	120	120
mA	160	160	170	170
Slice Thickness (unit)	5	5	5	5
Scan mode	Helical	Helical	Helical	Helical
Pitch (unit)	0.88	0.88	1.68	1.68
Scan length (mm)	S78.000-I77.000	S79.750-I85.250	S76.000-I89.000	S68.000-I97.000
Rotation time (s)	0.5	0.5	0.5	0.5
Center C				
kV		120		120
mA		68		68
Slice Thickness (unit)		3.75		3.75
Scan mode		Axial		Helical
Pitch (unit)		1		1.5
Scan length (mm)		S94.750-I80.250		S136.250-I115.000
Rotation time (s)		0.8		0.8
Center D				
kV		120		120
mA		81		160
Slice Thickness (unit)		5		5
Scan mode		Axial		Helical
Pitch (unit)		0.75		0.75
Scan length (mm)		S86.750-I103.250		S111.250-I126.750
Rotation time (s)		2		0.7

Table 3. Thermoluminescent dosimeter readings for the computed tomography phantoms.

Phantom	Centers	Protocol	Center(mGy)	Peripheral (mean) (mGy)	$CTDI_{vol}$ (mGy)
Standard head					
	A	Adult head	41.84	43.40	66.97
	B	Adult head	15.12	23.14	23.39
Constructed head					
	A	Adult head	40.15	41.28	63.91
	B	Adult head	22.73	21.01	24.67
	C	Adult head	7.52	10.6	9.57
	D	Adult head	22.4	19.46	27.16
Standard body					
	A	Adult body	23.45	15.57	21.85
	B	Adult body	11.12	10.25	6.29
Constructed body					
	A	Adult body	18.53	15.43	19.84
	B	Adult body	11.15	10.26	6.3
	C	Adult body	11.9	9.75	6.98
	D	Adult body	6.81	4.91	7.12

Table 4. Comparison of console displayed $CTDI_{vol}$ and DLP values for standard phantom with that of the locally constructed phantom for head and abdomen.

Protocols	Centers	Console $CTDI_{vol}$ (mGy)	Console $CTDI_{vol}$ (mGy)	% deviation	Console DLP (mGy.cm)	Console DLP (mGy.cm)	% deviation
		SP	CP		SP	CP	
Adult head							
	A	72	75.3	4.58	1663.1	2002.4	20.4
	B	26.82	27.98	4.33	471.75	520.1	10.25
Adult body							
	A	22.8	22.8	0	1066.8	975.6	-8.55
	B	7.55	7.75	2.65	140.72	144.54	2.72

SP= standard phantom, CP= constructed phantom

Table 5. Comparison of the uncertainty $CTDI_{vol}$ between the standard phantom with that of the locally constructed phantom for head and body.

Protocol	Centers	Estimated $CTDI_{vol}$	Estimated $CTDI_{vol}$	% deviation
		SP (mGy)	CP (mGy)	
Adult head				
	A	66.97	63.91	4.57
	B	23.39	24.67	5.47
Adult body				
	A	21.85	19.84	9.20
	B	6.29	6.30	0.00

SP= standard phantom, CP= constructed phantom

Table 6. Comparison of console displayed $CTDI_{vol}$ values with that of estimated $CTDI_{vol}$ for head and body with standard phantom.

Protocol	Centers	Standard phantom	Standard phantom	% deviation
		Console $CTDI_{vol}$ (mGy)	Estimated $CTDI_{vol}$ (mGy)	
Adult head				
	A	72	66.97	6.99
	B	26.82	23.39	12.79
Adult body				
	A	22.8	18.75	17.76
	B	7.55	6.29	16.69

Table 7. Comparison of console displayed $CTDI_{vol}$ values with that of estimated $CTDI_{vol}$ for the head with the locally constructed phantom.

Protocol	Centers	Constructed phantom	Constructed phantom	% deviation
		Console $CTDI_{vol}$ (mGy)	Estimated $CTDI_{vol}$ (mGy)	
Adult head				
	A	75.3	63.91	15.13
	B	27.98	24.67	11.83
	C	10.89	9.57	12.12
	D	27.59	27.16	3.57
Adult body				
	A	22.8	19.84	12.98
	B	7.75	6.3	18.7
	C	8.19	6.98	14.77
	D	7.48	7.12	4.81

The console displayed $CTDI_{vol}$ values and estimated $CTDI_{vol}$ for the standard head phantoms for center A were 72 and 66.97 mGy respectively [Table 6]. The console displayed $CTDI_{vol}$ values and estimated $CTDI_{vol}$ for the standard head phantoms for center B were 26.82 and 23.39 mGy respectively [Table 6]. The console displayed $CTDI_{vol}$ and estimated $CTDI_{vol}$ values for the standard body phantoms for center A were 22.8 mGy and 18.75 mGy. The console displayed $CTDI_{vol}$ and estimated $CTDI_{vol}$ values for the standard body phantoms for center B were 7.55 and 6.29 mGy. There was no difference between the $CTDI_{vol}$ from the console and that estimated from the TLD chips for the head of the standard phantom (P = 0.905). Similarly, there was no difference between the $CTDI_{vol}$ from the console and measured dose from the TLD chips for the body standard phantom (P = 0.813) [Table 6].

The console displayed $CTDI_{vol}$ values and estimated $CTDI_{vol}$ for the constructed head phantom for centers A, B, C and D were A (75.3 and 63.91) mGy, B (27.98 and 24.67mGy), C(10.89 and 9.57 mGy), and D(27.59 and 27.16mGy) respectively. The console displayed $CTDI_{vol}$ and estimated $CTDI_{vol}$ values for the constructed body phantom for centers A, B, C and D were A (22.8 and 19.84) mGy, B (7.75 and 6.3mGy), C (8.19 and 6.98 mGy), and D (7.48 and 7.12 mGy) respectively.

There was no difference between the $CTDI_{vol}$ from the console and the estimated values from the TLD chips for the head of the designed phantom (P = 0.380). Similarly, there was no difference between the $CTDI_{vol}$ from the console and measured dose from the TLD chips for the body designed phantom (P = 0.774) [Table 7].

Discussion

The uncertainty between the SP and CP with the head and body for centers A and B was within ±20%. Similarly, the console uncertainty between the SP and CP with the head and body for centers A and B was also within ±20%. A self-test of the constructed phantom for head and body shows that the maximum console $CTDI_{vol}$ and estimated $CTDI_{vol}$ with the TLD chips was <±20%. The uncertainty of the displayed console $CTDI_{VOL}$ of the standard and constructed phantom for the head and body of centers A and B was < ±5%, while the TLD measurements for the head and body was < ±6%. Generally, the displayed console doses were higher with the constructed phantom compared to the standard phantom. Also, the estimated dose values were higher for the body of the CP compared to that of the SP. A major reason for this could be in the design and accuracy of the locally made phantom compared to the generally accepted PMMA phantom. Nevertheless, the results obtained from the locally made phantom proved useful alongside those of the PMMA standard phantom.

The results from this study were in line with the American College of Radiology (ACR) quality control manual CTAP reference value of ±20%. The ACR recommendation also states that percent deviation could increase to ±30-40% based on the manufacturer's specified tolerance limit [16, 17]. Similarly, the obtained percent deviation in this study was within the IAEA acceptable limit of ±20% [19]. In addition, this study met the achievable criteria of ±10% set by the IAEA [19].

A study by Akpochafor et al., which developed a local phantom for dose verification, shows that the variation in doses between the standard and constructed head was ±15.2% [18]. This was higher than the variation in our study, which averaged to ±5%. Also, the percent deviation between the standard and constructed body phantom from Akpochafor's study was 5.3%, which was lower than that of our study, which averaged to ±9%. In most cases the variation between both results is largely dependent on the calibration factors of the TLDs, temperature conditions of the chips, uncertainty of the reader, and many other factors [10, 19]. It is worthwhile to note that the displayed console dose is only an estimate from a cylindrical phantom of the CT algorithm, which assumes the patient size. In reality, the displayed console dose is not the same as the real patient dose. The mathematical computation from the displayed console dose (mGy) and TLD measured dose (mGy) with bot head and body phantom were seen to be within ±20% [19].

Conclusion

Our study has successfully verified the accuracy of the dose delivered with both the standard and locally constructed phantoms. The findings revealed that the uncertainty between both phantoms with TLD measurements was within the ±10% achievable criteria limit. The displayed console $CTDI_{vol}$ was within the ±20% acceptable criteria limit, proving the validity of the new phantom. Correction factors for the head and body were 0.998 and 1.05 respectively, which makes the phantom valid. With the above validation, the locally designed phantom can be used for CT dose assessment and for dosimetry measurements.

Acknowledgments

The authors acknowledge with thanks the management and staff of each of the radiological centres covered, the Lagos State University radiation monitoring unit, and the management and staff of the National Institute of Radiation Protection and Research (NIRPR), Ibadan.

Conflicts of interest

The authors report no conflicts of interest.

References

1. Foley SJ, McEntee MF, Rainford LA. Establishment of CT diagnostic reference levels in Ireland. British J Radiol.2012; 85 (1018): 1390-1397. Available from https://doi.org/10.1259/bjr/15839549

2. Jurik AG, Nagel HD. Radiation exposure in computed tomography: fundamentals, influencing parameters, dose assessment, optimisation, scanner data, terminology. Eur Radiol. 2001; 11:2644. Available from https://doi.org/10.1007/s00330010108

3. Liguori C, Frauenfelder G, Massaroni C, et al. Emerging clinical applications of computed tomography. Med Devices (Auckl). 2015; 8:265-278. Available from https://doi.org/10.2147/MDER.S70630

4. Power SP, Moloney F, Twomey M, James K, O'Connor OJ, Maher MM. Computed tomography and patient risk: Facts, perceptions and uncertainties. World J Radiol. 2016; 8(12):902-915. Available from https://doi.org/10.4329/wjr.v8.i12.902

5. Adejoh T, Nzotta CC, Aronu ME, Dambele MY. Diagnostic reference levels for computed tomography of the head in Anambra State of Nigeria. West Afr. J Radiol. 2017; 24:142-6. Available from https://doi.org/10.4103/1115-3474.206806

6. Korir GK, Wambani JS, Korir IK, Tries MA, Boen PK. National diagnostic reference level initiative for computed tomography examinations in Kenya. Radiat Prot Dosimetry. 2016; 168(2), 242-252. Available from https://doi.org/10.1093/rpd/ncv020

7. Hasford F, Van Wyk B, Mabhengu T, Vangu MD, Kyere AK, Amuasi JH. Determination of dose delivery accuracy in CT examinations. J Radiat Res Appl Sc. 2015; 8(4): 489-92. Available from https://doi.org/10.1016/j.jrras.2015.05.006

8. Smith-Bindman R, Lipson J, Marcus R, Kim KP, Mahesh M, Gould R, et al. Radiation dose associated with common computed tomography examinations and the associated lifetime attributable risk of cancer. Arch Intern Med. 2009; 169(22):2078-2086. Available from https://doi.org/10.1001/archinternmed.2009.42

9. Coeytaux K, Bey E, Christensen D, Glassman ES, Murdock B, Doucet C. Reported Radiation Overexposure Accidents Worldwide, 1980-2013: A Systematic Review. PLoS ONE. 2015; 10(3): e0118709. Available from https://doi.org/10.1371/journal.pone.011870

10. Akpochafor M, Adeneye SO, Ololade Kehinde, Omojola AD, Oluwafemi A, Nusirat A, Aderonke A, Aweda MA, Bright Aboyewa O. Development of Computed Tomography Head and Body Phantom for Organ Dosimetry. Iran J Med Phys. 2019; 16:8-14.

11. Albngali A, Shearer A, van der Putten W, Tuohy B, Colgan N. CT Output Dose Performance-Conventional Approach Verses the Dose Equilibrium Method. IJMPCERO.2018; 7, 15-26. Available from https://doi.org/10.4236/ijmpcero.2018.71002

12. Descamps C, Gonzalez M, Garrigo E, Germanier A, Venencia D. Measurements of the Dose Delivered during CT Exams using AAPM Task Group Report No. 111. Journal of Applied Clinical Medical Physics. 2012; 13, 3934-3942. Available from https://doi.org/10.1120/jacmp.v13i6.3934

13. Xu J, He X, Xiao H, Xu J. Comparative Study of Volume Computed Tomography Dose Index and Size-Specific Dose Estimate Head in Computed Tomography Examination for Adult Patients Based on the Mode of Automatic Tube Current Modulation. Med Sci Monit. 2019; 25:71-76. Available from https://doi.org/10.12659/MSM.913927

14. Sadril L, Khosravi H.R. Setayeshi S. Assessment and evaluation of patient doses in adult common CT examinations towards establishing national diagnostic reference levels. Int. J Radiat. Res. 2013; 11: 245-252.

15. American Association of Physicists in Medicine (AAPM). Size-specific dose estimate (SSDE) in pediatric and adult body CT examinations. Report of AAPM Task Group 204. AAPM Publishing, College Park MD. 2011.

16. American College of Radiology (ACR). Computed tomography quality control manual. ACR publication. 2017; 78-81.

17. Samei E, Pfeiffer DE. Clinical imaging physics: Current and emergency practice. 1st Ed. John Wiley & Sons, Inc. West Sussex, UK. 2020. Available from https://doi.org/10.1002/9781118753798

18. Akpochafor MO, Adeneye SO, Habeebu MY, Omojola AD, Adedewe NA, Adedokun AR, Joseph AO, Ajibade OS, Etim VE, Aweda MA. Organ Dose Measurement in Computed Tomography Using Thermoluminescence Dosimeter in Locally Developed Phantoms. Iran J Med Phys 2019; 16: 126-132.

19. International Atomic Energy Agency (IAEA): Quality Assurance Programme for Computed Tomography: Diagnostic and Therapy Applications. IAEA Human Health Series No. 19. IAEA Publication, Vienna. 2012.